CHALMERS
UNIVERSITY OF TECHNOLOGY

Experimental investigation of chemical-looping combustion and chemical-looping gasification of biomass-based fuels using steel converter slag as oxygen carrier

Experimental investigation of chemical-looping combustion and chemical-looping gasification of biomass-based fuels using steel converter slag as oxygen carrier

Patrick MOLDENHAUER*, Carl LINDERHOLM, Magnus RYDÉN, Anders LYNGFELT

Chalmers University of Technology, Division of Energy Technology, 412 96 Gothenburg, Sweden
* Corresponding author: patrick.moldenhauer@chalmers.se, +46 (0)31 772 1469

Abstract – Chemical-looping combustion (CLC) is a combustion process with inherent separation of CO_2, which is achieved by oxidizing the fuel with a solid oxygen carrier rather than with air. As fuel and combustion air are never mixed, no gas separation is necessary and, consequently, there is no direct energy penalty for the separation of gases. The most common form of design of chemical-looping combustion systems uses circulating fluidized beds, which is an established and widely spread technology.

Experiments were conducted in two different laboratory-scale CLC reactors with continuous fuel feeding and nominal fuel inputs of 300 W_{th} and 10 kW_{th}, respectively. As oxygen carrier material, ground steel converter slag from the Linz–Donawitz process was used. This material is the second largest flow in an integrated steel mill, and it is available in huge quantities, for which there is currently limited demand. Steel converter slag consists mainly of oxides of Ca, Mg, Fe, Si and Mn. In the 300 W unit chemical-looping combustion experiments were conducted with model fuels syngas (50 vol% H_2 in CO) and methane at varied reactor temperature, fuel input and oxygen-carrier circulation. Further, the ability of the oxygen-carrier material to release oxygen to the gas phase was investigated. In the 10 kW unit, the fuels used for combustion tests were steam-exploded pellets and wood char. The purpose of these experiments was to study more realistic biomass fuels and to assess the lifetime of the slag when employed as oxygen carrier. In addition, chemical-looping gasification was investigated in the 10 kW unit using both, steam-exploded pellets and regular wood pellets as fuels.

In the 300 W unit, up to 99.9 % of syngas conversion was achieved at 280 kg/MW_{th} and 900 °C, while the highest conversion achieved with methane was 60 % at 280 kg/MW_{th} and 950 °C. The material's ability to release oxygen to the gas phase, i.e., CLOU property, was developed during the initial hours with fuel operation, and the activated material released 1-2 vol% of O_2 into a flow of argon between 850 °C and 950 °C. The material's initial low density decreased somewhat during CLC operation.

In the 10 kW, CO_2 yields of 75-82 % were achieved with all three fuels tested in CLC conditions, while carbon leakage was very low in most cases, i.e., below 1 %. With wood char as fuel, at a fuel input of 1.8 kW_{th}, a CO_2 yield of 92 % could be achieved. The carbon fraction of C_2-species was usually below 2.5 % and no C_3-species were detected. During chemical-looping gasification investigation a raw gas was produced that contained mostly H_2. The oxygen carrier lifetime was estimated to be about 110-170 h. However, due to its high availability and potentially low cost, this type of slag could be suitable for large-scale operation.

1 Introduction

1.1 Chemical-Looping Combustion and Chemical-Looping Gasification

Figure 1 shows illustrations of the chemical-looping combustion and chemical-looping gasification principles.

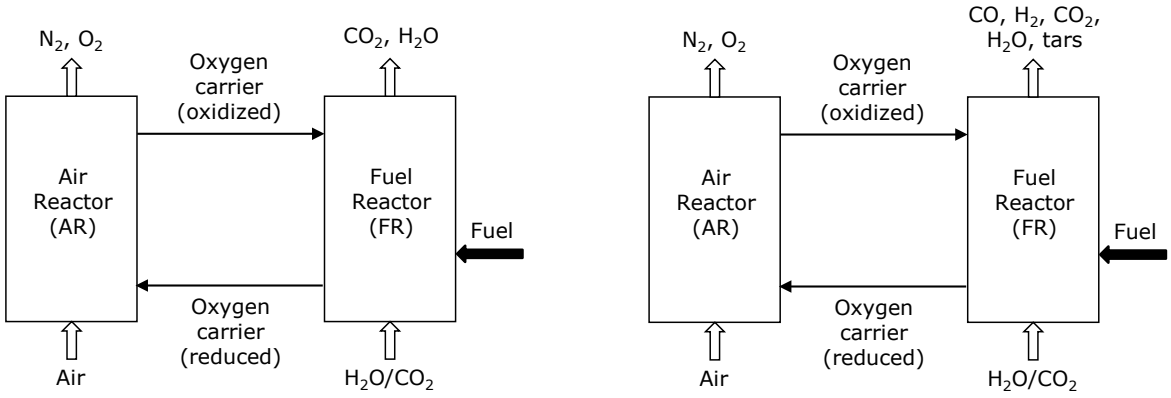

(a) CLC *(b) CLG*

Figure 1: Schematic illustrations of (a) chemical-looping combustion (CLC) and (b) chemical-looping gasification (CLG).

Chemical-looping combustion (CLC) is a carbon-capture technology with potential to drastically reduce the cost of CO_2 sequestration. The most common adaptation of CLC is based on two interconnected, chemical reactors: In the air reactor (AR) air is used to oxidize a solid oxygen-carrier, and in the fuel reactor (FR) fuel is added and oxidized by the oxygen carrier, which, in turn, is reduced. In this way, the combustion products are not diluted with nitrogen and, after condensation of steam, the fuel-reactor flue gas ideally consists of pure CO_2. In contrast to other carbon capture technologies, such as absorption or adsorption of CO_2 or oxyfuel combustion, there is no direct energy penalty for gas separation associated with chemical-looping combustion. General information about chemical-looping as well as an overview of trends and developments can be found elsewhere [1, 2].

Suitable process temperatures vary slightly for different oxygen-carrier materials, but are usually considered to be within the range of 850-1050 °C. The most commonly proposed way to design a chemical-looping combustor is to use circulating fluidized-beds (CFBs) with oxygen-carrier particles as bed material instead of an inert bed material as used in conventional applications.

In regular chemical-looping combustion, a gaseous fuel is assumes to react with the solid oxygen carrier. However, some oxygen-carrier materials can release gaseous oxygen, which was found to enhance fuel conversion. This process is referred to as chemical-looping with oxygen uncoupling (CLOU) [3].

The first CLC pilot, based on interconnected fluidized-bed technology, was constructed and commissioned in 2003. Today, chemical-looping operation in the literature involves at least 9000 h in 34 pilot units [4]. The majority of the operational experience with chemical-looping combustors has been obtained using gaseous fuels and manufactured oxygen carriers. In the case of chemical-looping combustion with solid fuels, however, more often low-cost materials based on minerals or waste materials are used. There are two main reasons for the focus on such low-cost materials. Firstly, solid

fuels usually contain significant quantities of ash, which is expected to decrease the life-time of the oxygen carrier. Secondly, the requirements with respect to reactivity of an oxygen carrier material for solid fuels tend to be lower as compared to hydrocarbon-based, gaseous fuels. This is due to the higher chemical stability of, for example, methane in natural gas in contrast to the more reactive gases CO and H_2, which are intermediate products in solid fuel conversion.

Chemical-looping gasification (CLG) is built around the same principles as indirect fluidized-bed gasification, with two interconnected fluidized beds – air reactor and fuel reactor/gasifier – but uses an oxygen carrier instead of sand as bed material. This has potential advantages as compared to normal indirect gasification. Firstly, a more oxidizing environment and the presence of oxygen carriers in the gasifier reduces the tar content. Secondly, the cost of gas cleaning is reduced, as essentially all the fuel is converted in the fuel reactor, and none in the air reactor, thus reducing the volume of gas needing clean-up. Moreover, as no CO_2 is expected from the air reactor the CO_2 stream is concentrated with the syngas and, hence, amiable for capture. If biomass is used as fuel and capture of the CO_2 is applied, negative emissions of CO_2 can be achieved, while at the same time producing valuable syngas that can be used for, for example, biofuel production.

In this work, the CLC and CLG processes are made more cost-effective by using a by-product from the steel industry as oxygen carrier material.

2 Experimental

2.1 Chemical-Looping Test Units

2.1.1 300 W Unit

The laboratory-scale continuous 300 W unit requires approximately 250-400 g of oxygen-carrier particles, depending on their density. The reactor is 300 mm high and has two reactor chambers: an air reactor fluidized with air and a fuel reactor fluidized with methane. The fuel reactor has a cross-section of 25 mm x 25 mm, whereas the base of the air reactor is 25 mm x 42 mm and contracts to 25 mm x 25 mm in the riser section. Figure 2 shows the working principle of the reactor unit: high gas velocities cause the particles to leave the air reactor and enter the gas-solid separator placed on top flange of reactor unit (not shown). The particles fall back and enter the inlet of the J-type loop seal (downcomer). This causes particles at the outlet of the loop seal to drop down onto the bubbling bed of the fuel reactor (through the return orifice). From the bottom of the fuel reactor the particles flow back into the air reactor via the lower loop-seal. The air reactor is fluidized with air, the loop seals are fluidized with argon and the fuel reactor is fluidized with either methane (fuel operation) or argon (determination of CLOU behavior).

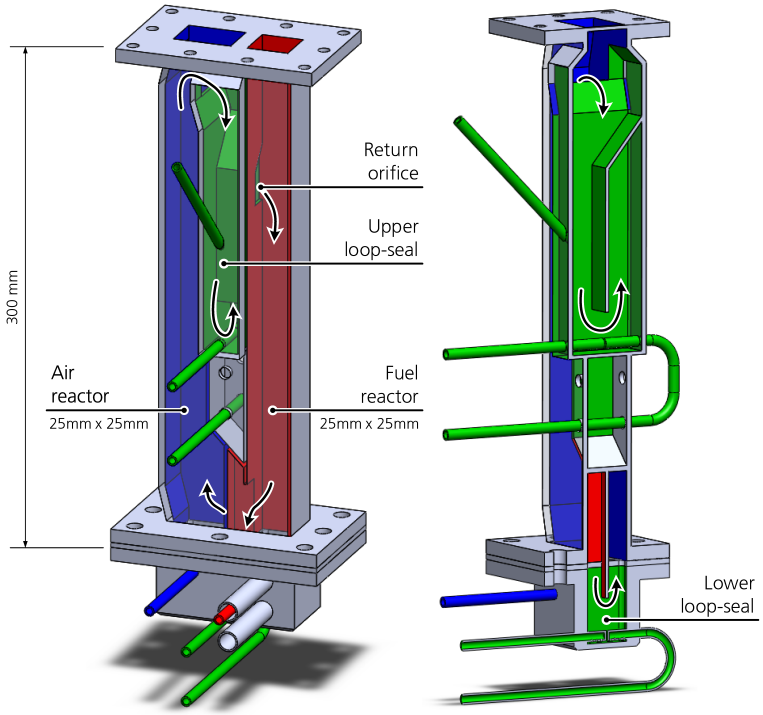

Figure 2: Illustration of the 300 W chemical-looping combustion reactor.

The off-gases from the reactors are separately cooled to 4 °C and filtered. The fuel-reactor flue gas passes a water seal, which generates a slight over pressure in the fuel reactor and reduces leakage of air from into the fuel reactor. The dried gases are analyzed for CO, CO_2, CH_4 (IR sensors) and O_2 (paramagnetic sensor). The fuel-reactor flue gas is also analyzed in a gas chromatograph to verify these gas species and to further quantify N_2 and H_2.

2.1.2 10 kW Unit

The 10 kW CLC unit consists of a fuel reactor (FR), an air reactor (AR), a riser, a cyclone and loop seals. In the fuel reactor the fuel is gasified by steam, whereupon gasification products are oxidized by the oxygen carrier, which, in turn, is reduced. The fuel reactor is also equipped with a recirculation loop, which is not shown in Figure 3, the function of which is to return elutriated char particles to the fuel reactor. In the air reactor (AR) the oxygen carrier is oxidized. In the riser, the oxygen carrier particles are lifted and circulated back to the fuel reactor via the cyclone – a gas–solids separator – and the upper loop-seal. The upper and lower loop-seals inhibit gas leakages between air reactor and fuel reactor.

The fuel reactor is fluidized with steam and operated as a bubbling bed. The fuel is introduced 100 mm into the bed, and the total bed height, i.e. the distance from the gas distribution plate to the overflow exit, is 273 mm. The fuel reactor has an internal partitioning to prevent surface by-pass and, consequently, give the particles a more even residence-time distribution. The total solids inventory is around 15 kg, out of which approximately 5 kg are in the fuel reactor. A schematic of the unit is shown in Figure 3. A more detailed description of the 10 kW unit can be found elsewhere [5].

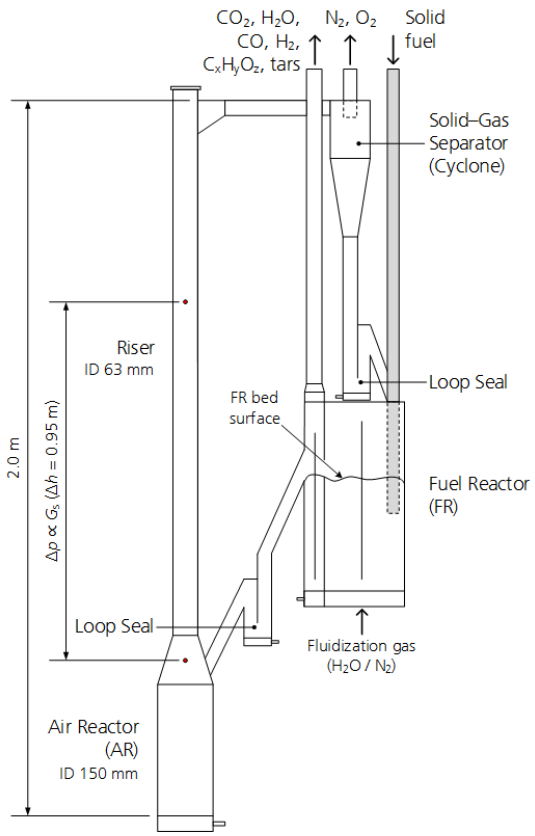

Figure 3: Schematic of the 10 kW chemical-looping reactor. The measured pressure difference along the riser section, which is assumed to be proportional to the solids circulation, G_s, is shown. The recirculation loop connected to the fuel reactor is not shown.

The reactor is placed in an electrically heated furnace, which is necessary in order to reach the desirable operating temperatures at start-up. Due to heat losses from the system, heat also needs to be supplied to the reactor system during normal operation with fuel.

After passive cooling in finned pipes, the air reactor flue gas passes through a textile filter, where elutriated particles are trapped. The fuel-reactor flue gas is led through a water seal, which generates a slight overpressure in the fuel reactor with the purpose to control the pressure balance of the reactor system.

Cleaned and dried gas samples from both chimneys are led to gas analysers, where the fractions of O_2 and CO_2 are determined in the flue gas of the air reactor, and, respectively, the fractions of CO_2, CO, CH_4, O_2, and H_2 in the flue gas of the fuel reactor. The instruments used are Rosemount NGA2000 and Sick Sidor. CO_2, CO and CH_4 are measured by IR sensors, O_2 with a paramagnetic sensor and H_2 with a thermal conductivity sensor. Bronkhorst mass flow controllers regulate all incoming gas flows and pressure transducers are used to monitor differential pressures related to bed heights and particle flows. Temperature in the system is monitored by three K-type thermocouples that are located in the air reactor, in the cyclone and in the fuel reactor.

2.2 Oxygen Carrier Material

Important criteria for oxygen carriers used in chemical looping with solid fuels include:

- high reactivity with fuel and oxygen, and ability to convert the fuel fully to CO_2 and H_2O
- physical integrity during long periods of operation

- low cost
- preferably being environmentally sound

Combustion of solid fuels inevitably involves the release of fuel ash, which means that a large mass flow of ash has to be continuously discharged. This ash discharge, and possibly also fouling by ash, is expected to limit the lifetime of the oxygen carrier. Consequently, oxygen carriers of low cost are the primary choice for chemical-looping combustion and chemical-looping gasification with solid fuels. Natural minerals are such a low-cost option for oxygen carriers, industrial by-products like LD slag are another option. The feasibility of using minerals as oxygen carriers in CLC has previously been investigated and demonstrated [5-8].

LD slag is the second largest by-product in steelmaking. It is formed by reactions of slag formers (e.g. burned lime), silica, iron and other components during conversion of carbon-rich molten pig iron into steel in the basic oxygen blown converter process (aka Linz-Donawitz process). A typical steel mill may generate 100-300 kton/year, of which less than half can be recirculated internally to the blast furnace. There is very limited demand for LD slag for other purposes.

The chemical composition of LD slag makes it interesting as oxygen carrier. The composition will depend on the raw material used. A recent analysis from our source: 26.6 % Fe_2O_3, 3.3 % MnO, 11.9 % SiO_2, 39.8 % CaO, 9.1 % MgO with oxides of aluminum, titanium and vanadium being the main impurities. It shall be noted that combined Fe-Mn-Si oxides are among the more interesting combined oxide systems for oxygen carrying purposes [9, 10]. LD slag has previously been examined as oxygen carriers in experiments involving combustion [11] and tar reforming [12].

LD slag is generated after the molten steel have been tapped off from the converted vessel. The remaining molten slag is then poured into a slag pot which subsequently is discharged outside. LD slag is formed during cooling and solidification of the melt. The resulting slag is rather homogenous and possibly of more predictable quality than virgin minerals. It has high skeletal density (3 500 kg/m^3) but its bulk density (1 200-1 400 kg/m^3) is similar to that of sand.

The LD slag used for these experiments was produced by SSAB Merox AB. A sample of 180 tons was taken from a storage pile containing about than 1 million tons. The sample was dried, crushed and sieved in a sieve shaker using two sieves (400 μm and 100/150 μm). The result was 38 tons of particulate LD slag in the size range 100-400 μm, to be used in a number of research activities.

2.3 Fuels used

For the tests conducted in the 300 W unit the fuels used were syngas, i.e., 50 vol% H_2 in CO, and methane.

The fuels used for chemical looping combustion and chemical looping gasification in the 10 kW unit are wood char, wood pellets, and steam-exploded wood pellets (aka black pellets). The wood char is produced by heat treatment (≈ 450 °C for > 10 h) in inert atmosphere. The steam-exploded wood pellets are intended for co-firing with coal and produced by exposing woody biomass to pressurized steam followed by a sudden pressure release and pelletization.

A major difference between the fuels is the volatile content. Volatiles are released quickly upon heating of the particles, and fuels rich in volatiles can create gas bubbles, which pass through the bed too quickly to be fully converted. The volatile content of the different fuels used as well as other properties are shown in Table 1.

Table 1: Properties of the solid fuels used for investigations in the 10 kW unit.

	Swedish wood char	Wood pellets	Steam-exploded wood pellets
Alternate notation	Wood char	Crushed wood pellets, sawdust	Black pellets, heat-treated stem wood
Producer	Skogens Kol	n/a	Arbaflame
LHV (MJ/kg)	29.8	17.7	18.6
Size, d_{50} (mm)	0.8	0.6	1.6
Proximate analysis (mass%, as received)			
Fixed carbon	73.9	15.1	18.7
Volatiles	16.7	78.4	74.2
Moisture	3.9	6.0	6.9
Ash	5.5	0.5	0.3
Ultimate analysis (mass%, daf)			
C	86.9	47.6	53.5
H	3.2	5.6	6.0
O	9.5	40.2	40.3
N	0.4	0.1	0.1
S	0.03	0	0
Chemical-looping operation investigated	CLC	CLC, CLG	CLC, CLG
Total amount of fuel added (g)	2 430	850	14 760
Fuel operation time (h)	5.1	21.6	1.2

LHV … lower heating value
daf … dry and ash free

The size of the fuel particles affects both the reactivity and fluid-dynamic properties of the particles. Small particles gasify faster due to a higher surface-to-volume ratio. On the other hand, small particles tend to follow the gas stream, whereas larger particles are likely to remain in the bed for longer periods of time. Hence, use of small fuel particles decreases fuel residence time in the bed, which can lead to lower solid-fuel conversion. A carbon stripper can be used to separate fuel and oxygen-carrier particles, if there is a sufficient difference in terminal velocity between the two types of particles.

2.4 Definitions and Data Evaluation

2.4.1 300 W unit

The ability of an oxygen carrier to convert fuel to CO_2 is expressed by the CO_2 yield γ_{CO2}, see Equation (1), where $[i]_{FR}$ are the volume fractions of species i measured in the fuel reactor. The calculation is based on a carbon balance over the fuel reactor outlet.

$$\gamma_{CO2} = \frac{[CO_2]_{FR}}{[CO_2]_{FR} + [CO]_{FR} + [CH_4]_{FR}} \quad (1)$$

2.4.2 10 kW unit

Solids circulation

One way to quantify the circulation of solids in a circulating fluidized-bed (CFB) reactor is through the mass flux of solids, G_s, which expresses the circulation as mass flow per area in kg/m^{2}s. Normally, the cross-sectional area of the riser is used as reference. This allows for comparison of solid circulation

of CFB units of different size. It is usually not possible to measure the mass flux of solids directly, which is why it is calculated based on pressure measurements, which are extrapolated in order to obtain the bed density at the exit of the riser [13]. For practical reasons, this estimation is further simplified and adapted to the 10 kW unit, see Equation (2). CI is referred to as circulation index and is based on a pressure measurement over the riser, cf. Figure 3, on the superficial gas velocity, u_0, and on the terminal velocity, u_t, which is approximated according to Kunii & Levenspiel [14]. Hence, the circulation index represents the gross amount of particles in the chosen riser segment, i.e., the sum of particles travelling upwards and downwards, and gives an overestimation of the true mass flux of solids. The circulation index is assumed to be proportional to the real mass flux.

$$\mathrm{CI} = -\frac{1}{g} \cdot \frac{\Delta p}{\Delta h} \cdot (u_0 - u_t) \tag{2}$$

Fuel conversion
Fuel that enters the fuel reactor can follow one of three routes:

1. Conversion to gas in the fuel reactor, which is the desired case.
2. Conversion in the air reactor. Some char will inevitably follow the flow of oxygen carrier to the air reactor, where it is oxidized to CO_2. This is expressed by Equation (3).
3. Exit the fuel reactor via the chimney as unconverted char (not monitored).

Gaseous species produced in the fuel reactor are either volatile fuel-compounds or products of char gasification. Volatiles include mainly CH_4, H_2, CO and CO_2. Higher hydrocarbons are also present to smaller extent, but these are only measured up to C_3H_8.

The degree och fuel oxidation, η_{fuel}, is the ratio of the amount of oxygen consumed by the oxygen carrier in the air reactor with the stoichiometric amount of oxygen needed for full conversion of fuel to CO_2 and H_2O. Equation (3) shows how the degree of fuel oxidation is calculated.

$$\eta_{\mathrm{fuel}} = \frac{\dot{n}_{\mathrm{O2,OC,AR}}}{\dot{n}_{\mathrm{O2,stoich}}} = \frac{\dot{n}_{\mathrm{O2,AR,in}} - \dot{n}_{\mathrm{O2,AR,out}} - \dot{n}_{\mathrm{CO2,AR,out}}}{\dot{n}_{\mathrm{O2,stoich}}} \tag{3}$$

Based on the concentration of CO_2 in the exhaust gases from the air reactor the fraction of fuel carbon that leaks into the air reactor, $f_{\mathrm{C,AR}}$, is determined, see Equation (4). The flow of CO_2 leaving the air reactor is compensated for the atmospheric concentration of CO_2, which was approximately 400 ppm during the time of the experiments. Closely connected to this carbon leakage is the carbon capture efficiency, η_{CC}, which reflects unconverted char reaching the air reactor and being oxidized to CO_2, see Equation (5). The carbon capture efficiency is the ratio of the carbon that leaves the fuel reactor via the chimney, i.e., converted to gas or as char, to the total flow of carbon into the reactor system.

$$f_{\mathrm{C,AR}} = \frac{\dot{n}_{\mathrm{CO2,AR,out}}}{\dot{n}_{\mathrm{C,fuel}}} \tag{4}$$

$$\eta_{\mathrm{cc}} = 1 - f_{\mathrm{C,AR}} \tag{5}$$

Another way to evaluate the conversion of fuel, which gives more detailed information about the different steps of conversion and selectivity, is to quantify the different species in the exhaust gas of the fuel reactor. The measurement equipment used, cf. Section 2.1.2, allows for monitoring of hydrocarbons up to C_3H_8. The different carbon species are distinguished and calculated according to

Equations (6)-(10). A special denotation was chosen for the fraction of CO_2, i.e., γ_{CO2}, to highlight that this is the desired carbon fraction.

$$\gamma_{CO2} = \frac{\dot{n}_{CO2,FR}}{\dot{n}_{CO2,FR} + \dot{n}_{CO,FR} + \sum_x (x \cdot \dot{n}_{CxHy,FR})} \quad (6)$$

$$f_{CO} = \frac{\dot{n}_{CO,FR}}{\dot{n}_{CO2,FR} + \dot{n}_{CO,FR} + \sum_x (x \cdot \dot{n}_{CxHy,FR})} \quad (7)$$

$$f_{CH4} = \frac{\dot{n}_{CH4,FR}}{\dot{n}_{CO2,FR} + \dot{n}_{CO,FR} + \sum_x (x \cdot \dot{n}_{CxHy,FR})} \quad (8)$$

$$f_{C2} = \frac{\dot{n}_{C2Hy,FR}}{\dot{n}_{CO2,FR} + \dot{n}_{CO,FR} + \sum_x (x \cdot \dot{n}_{CxHy,FR})} \quad (9)$$

$$f_{C3} = \frac{\dot{n}_{C3Hy,FR}}{\dot{n}_{CO2,FR} + \dot{n}_{CO,FR} + \sum_x (x \cdot \dot{n}_{CxHy,FR})} \quad (10)$$

The air-to-fuel ratio is the molar ratio of air fed to the air reactor and the stoichiometric amount of air needed for complete combustion of fuel, see Equation (11). A high air-to-fuel ratio also indicates a high circulation. The air-to-fuel ratios used in the 10 kW pilot unit are much higher than what would be feasible in a large-scale process. The reason for is that the 10 kW unit was designed for flexibility with respect to, e.g., oxygen carrier, fuel type and fuel input. The air flow in the riser is used to vary solids circulation and when high rates of solids circulation are tested together with a low fuel input, the air-to-fuel ratio reaches very high values. It was used for the evaluation of the results, because it expresses both, fuel flow and solids circulation in one value.

$$\mathrm{AFR} = \frac{\dot{n}_{O2,AR,in}}{\dot{n}_{O2,stoich}} \quad (11)$$

3 Results

3.1 Experiments in 300 W unit

3.1.1 CLOU properties

The CLOU effect of LD slag was determined at different residence times in the 300 W reactor, i.e., in the beginning of the campaign and at its end, see Figure 4. This was done by monitoring the oxygen released in the fuel reactor, which was fluidized with argon. The fresh material showed little to no CLOU effect as the concentration of released oxygen could not be clearly differentiated from oxygen that leaked into the fuel reactor, i.e., 0.3-0.6 vol%. The used material, however, showed a distinct CLOU effect and the released oxygen was clearly higher than oxygen due to leakage. The amount of oxygen released by the used material increased with increasing temperature and varied between 1.1 vol% and 1.7 vol% between 850 °C and 950 °C at a flow of 1 L_n/min of argon. It appears as if CLOU properties developed during the first day of fuel operation, i.e., 2.7 h of operation with syngas, which corresponds to about 85 redox cycles.

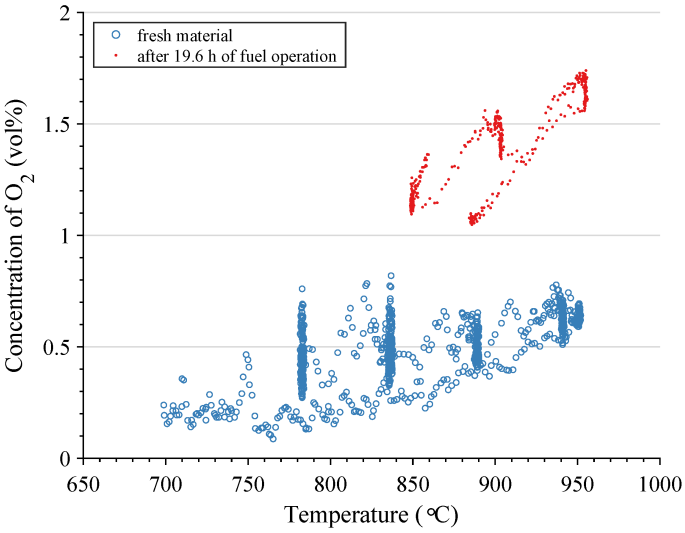

Figure 4: Oxygen release of LD slag oxygen carrier in inert atmosphere (1 L_n/min of argon) at varied temperature. The concentration of O_2 at the outlet of the air reactor was 18.2-18.5 vol% with the fresh material and 19.3-19.5 vol% with the material after fuel operation. Each data point represent a 10 s-average.

3.1.2 Fuel conversion

With syngas as fuel, a very high CO_2 yield, up to 99.9 mol%, was achieved at 900 C and a specific fuel-reactor bed mass of 280-340 kg/MW_{th}, see Figure 5a. Initially, however, fuel conversion at similar conditions was lower, i.e., 98.1-98.7 mol% at 270-365 kg/MW_{th}. This initial phase with lower fuel conversion lasted approximately a little more than 2 h. It seems likely that this improvement in fuel conversion is correlated to the development of CLOU properties described in Section 3.1.1. Syngas conversion with the LD slag-based oxygen carrier is higher than that of all but one manganese ore-based oxygen carriers tested in this unit; five materials published [6, 15] as well as four materials unpublished.

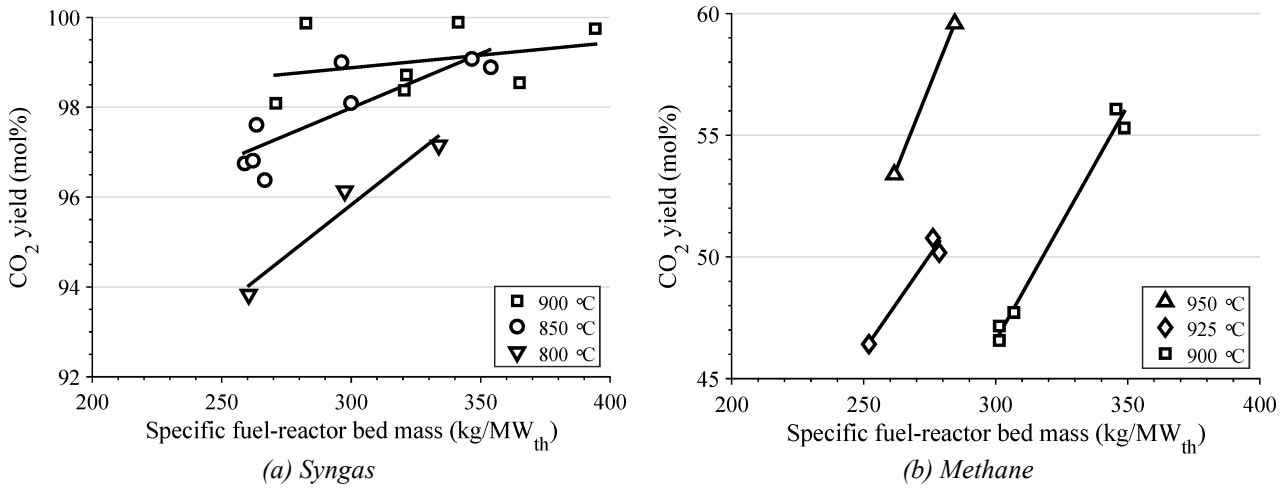

Figure 5: Fuel conversion, i.e., CO_2 yield γ_{CO2}, as a function of the specific fuel-reactor bed mass at different temperatures with (a) syngas and (b) methane as fuel.

Syngas conversion improved towards higher temperatures and higher specific fuel-reactor bed masses. Initially, experiments in the 300 W unit with LD slag as oxygen carrier were conducted with syngas as fuel at 900 °C. Therefore, the high degree of variation seen in the data points representing 900 °C is likely linked to the initial phase of material activation.

After fuel testing with syngas, a series of experiments was performed with methane as fuel, see Figure 5b. Fuel conversion varied clearly with temperature as well as with specific fuel-reactor bed mass; between 250 kg/MW_{th} and 350 kg/MW_{th}, and 900 °C and 950 °C, CO_2 yields between 46 mol% and

60 mol% were achieved. This is somewhat higher than fuel conversion achieved with most manganese ore-based oxygen carriers that were tested in this unit; four materials published [6, 15] as well as four materials unpublished.

3.1.3 Particle attrition and characteristics

Particle attrition was monitored during fuel operation in the 300 W unit, and, additionally, attrition behavior of fresh and used particles was analyzed in a customized jet-cup attrition rig [16]. The different attrition rates as well as fuel operation time, bulk density and particle size distribution are presented in Table 2. The bulk density decreased significantly despite a widening of the particle size distribution. This suggests that the decrease in particle density was higher than that of the bulk density.

Table 2: Particle attrition, fuel operation time, poured bulk density and particle size distribution.

Fuel operation	(h)	
Syngas		14.1
Methane		5.9
Average attrition rate observed under redox conditions	(wt%/h)	0.58
Attrition index measured in a customized jet-cup attrition rig	(wt%/h)	
Fresh particles		0.97
Particles after 20 h of fuel operation		6.2
Bulk density determined based on standard ISO 3923-1	(kg/m^3)	
Fresh particles		1180
Particles after 20 h of fuel operation		1000
Particle sizes D_{10}, D_{50}, D_{90}	(μm)	
Fresh particles		148, 180, 235
Particles after 20 h of fuel operation		62, 167, 224

3.2 Experiments in 10 kW unit

3.2.1 Fuel conversion

Table 3 shows the experimental parameters that were investigated with LD slag as oxygen carrier material.

Table 3: Experimental parameters investigated in the 10 kW unit with LD slag as oxygen carrier for the different fuels used.

		Black pellets	Wood char	Wood pellets
Superficial gas velocity in the Riser	(m/s)	2.8-5.5	3.1-4.9	2.6-4.7
Air reactor temperature	(°C)	815-940	820-920	825-935
Fuel reactor temperature	(°C)	920, 965-980	965-985	980-985
Fuel flow	(g/min)	9.0-33.5	3.0-6.6	6.6-14.8
	(kW_{th})	2.8-10.4	1.5-3.3	1.9-4.4
Air-to-fuel ratio	(mol/mol)	1.0-8.1	3.0-7.9	2.9-7.0
Hydrogen-to-carbon ratio	(mol/mol)	4.7-13.0	5.8-22.7	10.0-22.4
Bed mass in fuel reactor	(kg)	5-6	5-6	5-6
Total bed mass	(kg)	12-17	12-16	12-14
Estimated specific fuel-reactor bed mass	(kg/MW_{th})	500-2 100	4 000-5 300	1 100-3 200

A higher superficial gas velocity in the riser leads to a higher circulation index, see Figure 6. The gas velocity in the riser was always higher than the average terminal velocity of the particles, i.e., 0.5-

0.8 m/s. The relatively high variation of the circulation index for a given superficial gas velocity is likely a result of variations in the system inventory. In the gas–solids separator, a large amount of particles, not only fines, was elutriated from the system and, consequently, the system inventory varied between 12 kg and 17 kg, cf. Figure 11.

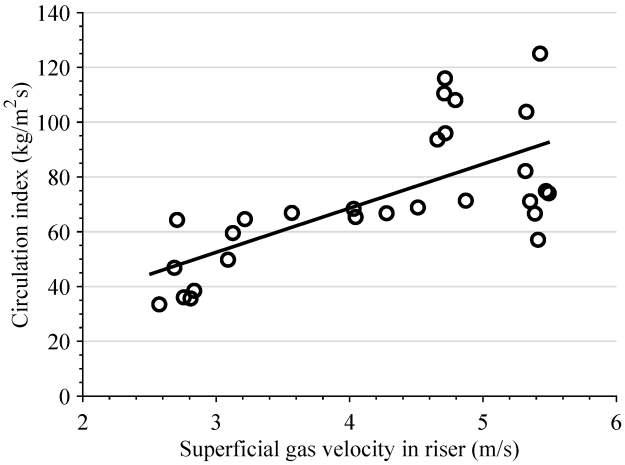

Figure 6: Circulation index at varied superficial gas velocity in the riser.

The degree of fuel oxidation and carbon leakage to the air reactor at varied air-to-fuel ratio for the different fuels used are shown in Figure 7 and Figure 8. The degree of fuel oxidation increases with an increasing air-to-fuel ratio. With black pellets at very high air-to fuel ratios high degrees of fuel oxidation were achieved, i.e., 92 % and 96 %. In most cases carbon leakage was below 1 % of the fuel carbon and, except for a few outliers, all leakage was below 20 %. Carbon leakage with wood char as fuel seems to be higher than with the other two fuels investigated. It should be noted that both, the degree of fuel oxidation and carbon leakage to the air reactor, contain rather high uncertainties that stem from the uncertainty when estimating the fuel flow, which is known to vary considerable at certain conditions. Therefore, the uncertainties for both, the degree of fuel oxidation and carbon leakage to the air reactor, are estimated to be up to 20 % of the respective values.

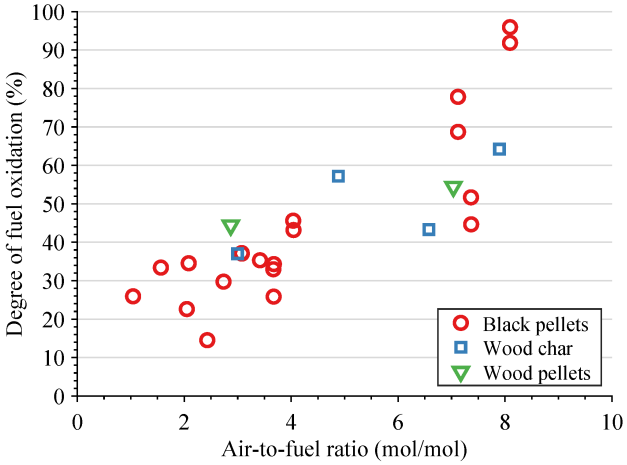

Figure 7: Degree of fuel oxidation at varied air-to-fuel ratio, i.e., at varied air- and fuel input. The degree of fuel oxidation does not include fuel oxidized in the air reactor. The fuel reactor temperature was 965-985 °C, except in one case with black pellets as fuel, at AFR = 3.4, when it was 920 °C. Values above 100 % are not shown.

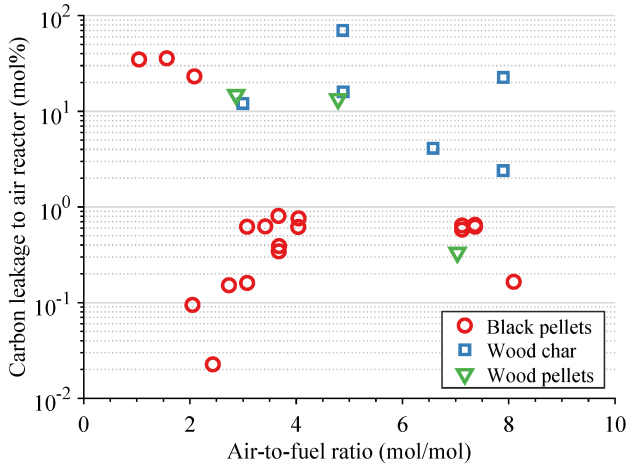

Figure 8: Carbon leakage to the air reactor at varied air-to-fuel ratio. The fuel reactor temperature was 965-985 °C, except in one case with black pellets as fuel, at AFR = 3.4, when it was 920 °C.

Figure 9a-Figure 9d show the different fractions of carbon species in the fuel reactor, γ_{CO2}, f_{CO}, f_{CH4} and f_{C2}, at varied air-to-fuel ratio for the different fuels used. No C_3-species were detected during any

of the experimental settings investigated. The highest CO_2 yield was achieved with wood char at a fuel input of 1.8 kW_{th}. Here, the CO_2 yield was 92 % and the carbon leakage was low, i.e., 2.4 %. Increasing the air-to-fuel ratio clearly improves fuel conversion, i.e., the CO_2 yield increases while the carbon fractions of C_2, CH_4 and CO decrease. When wood char was used as fuel, which has a low volatiles content, the CO_2 yield was generally somewhat higher than with black pellets or wood pellets but this could also be an effect of the higher carbon leakage. Further, the amount CH_4 was clearly lower than with black pellets or wood pellets and no C_2- or C_3-species were detected.

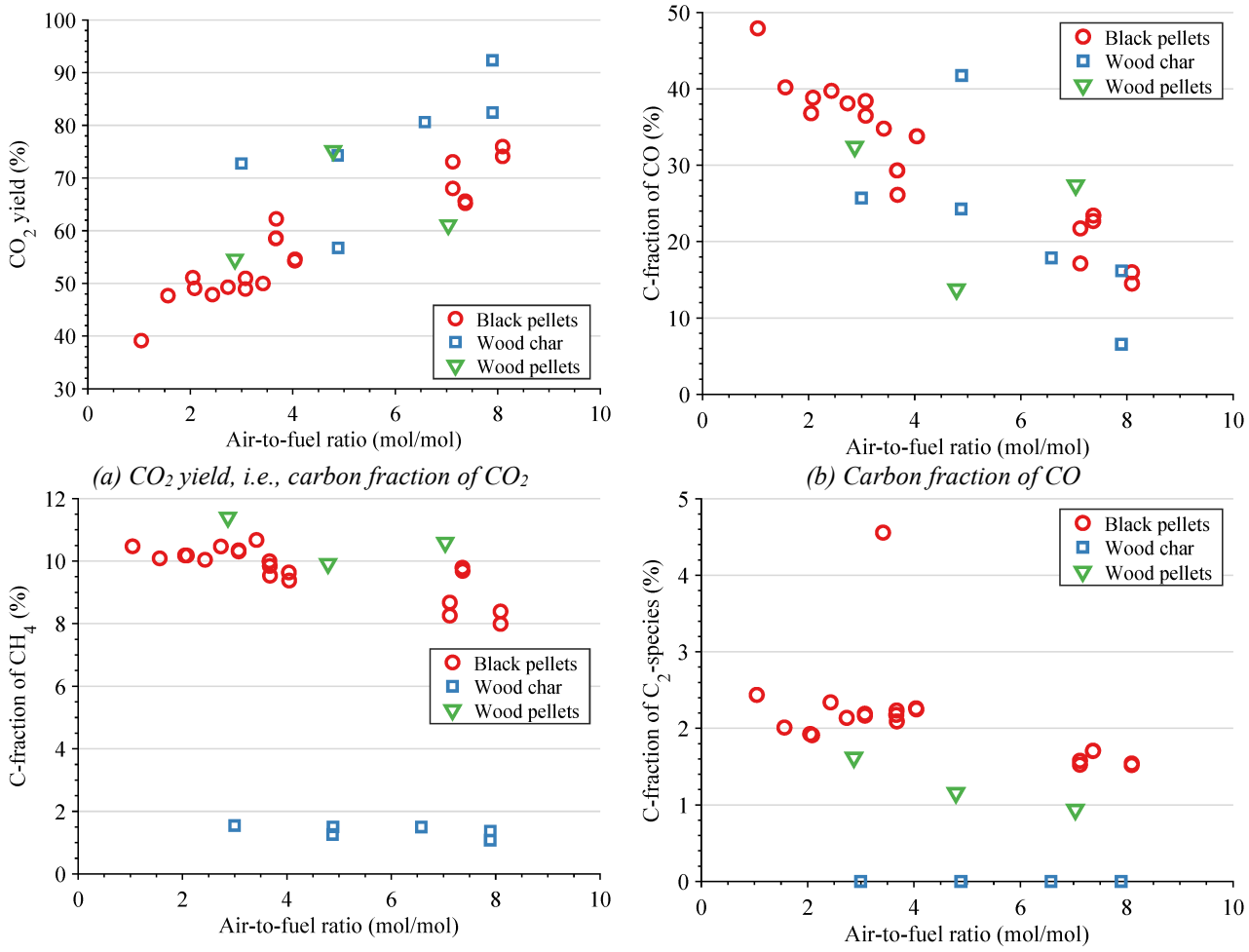

(a) CO_2 yield, i.e., carbon fraction of CO_2

(b) Carbon fraction of CO

(c) Carbon fraction of CH4

(d) Carbon fraction of C_2-species

Figure 9: Carbon fractions in the fuel reactor at varied air-to-fuel ratio for the different fuels used, (a) CO_2 yield, i.e., carbon fraction of CO_2, (b) carbon fraction of CO, (c) carbon fraction of CH_4 and (d) carbon fraction of C_2-species. No C_3-species were detected during any of the experimental settings investigated. The fuel reactor temperature was 965-985 °C, except in one case with black pellets as fuel, at AFR = 3.4, when it was 920 °C.

The concentration of hydrogen measured was clearly above that of carbon monoxide, which can be attributed to the high hydrogen-to-carbon ratio in the fuel reactor, i.e., 4.7-22.4. The fractions of hydrogen measured in the fuel-reactor flue gas follows the same trend as the carbon fractions of CO Figure 9b. The highest average concentration of hydrogen was 36 vol% and was detected at 6.9 kW_{th} fuel input of black pellets, at an air-to-fuel ratio of 1.6 and a hydrogen-to-carbon ratio of 6.4. The lowest hydrogen fraction measured was 6.6 vol%. There is no clear correlation for fuel type or hydrogen-to-carbon ratio.

3.2.2 Particle attrition and lifetime

Initially a large batch of LD slag based oxygen carrier was prepared, ca 30 kg, by removing particles larger than 500 µm followed by a washing process to remove fines, here defined as particles smaller than 63 µm. Thus the amount of fines in the fresh material was reduced to about 5 wt%. During operation, material was elutriated from both air reactor and fuel reactor at a rather high rate. Elutriated material was collected in the bag filter connected to the air reactor cyclone, in a horizontal pipe section between the fuel reactor outlet and the water-seal and in the water-seal. After fines were quantified and removed from the elutriated material, the fraction larger than 63 µm, together with fresh material, was refilled into the system. Fines were not collected continuously and the data was smoothed, i.e., interpolated.

The curve showing the cumulative amount of fines produced exhibits two jumps, at 4.3 h and at 8.9-9.4 h, see Figure 10. There, larger amounts of fresh material were added to the system. The rate of fines production is low during the initial four hours of fuel operation as well as during the last nine hours of fuel operation. In between, fines are produced at a higher rate, see Figure 11. Fresh oxygen carrier material, which contained about 5 wt% of fines, was added throughout the entire experimental campaign, see Figure 10, though more fresh material was added initially. Hence, the change in fines production over time is likely a result of several factors.

1. Fresh oxygen carrier contains about 5 wt% of fines. Whenever fresh material is added these fines are assumed to be elutriated instantly.
2. Fresh LD slag was found to undergo changes during the first hours of fuel operation, cf. Sections 3.1.1 and 3.1.2. This transition is likely to cause stresses within the material that lead to an increased attrition until the transition is complete.
3. Fines that are fuel ash can be neglected. 22.8 h of the total fuel operation was conducted with fuels that contained little ash, i.e., 49 g in total, and during 5.5 h wood char was used, which contained a total of 134 g ash.
4. Fines that are unconverted char were not quantified, but their influence on the fines production observed is assumed to be negligible. During the entire fuel operation time, the fuel added contained a total of fixed carbon of about 4.7 kg. If it is assumed that 5 % of that carbon left the fuel reactor as char, this would correspond to a fraction of 2.5 % of the total amount of fines produced.

It is assumed that the estimated average particle lifetime during the last part of the investigation, i.e., 110-170 h, is more representative for a large-scale operation. For a chemical-looping combustion boiler with a thermal power of 1000 MW, which contains a total of 850 t of solids inventory (500 t in the fuel reactor, 250 t in the air reactor and the rest in gas–solids separators and loop-seals) [17], the resulting regeneration rate of bed material would be in the range of 5-8 kg/MWh. It is emphasized that this number does not consider bed regeneration due to interaction with ash components, which may lead to sintering of the bed material. The typical regeneration rate of bed material used in conventional, biomass-fired CFB boilers is about 3 kg/MWh of quartz sand. If the interaction of an LD slag-based oxygen carrier with fuel ash is suitable and its cost is low, it can be a relevant oxygen-carrier material for large-scale chemical-looping combustion.

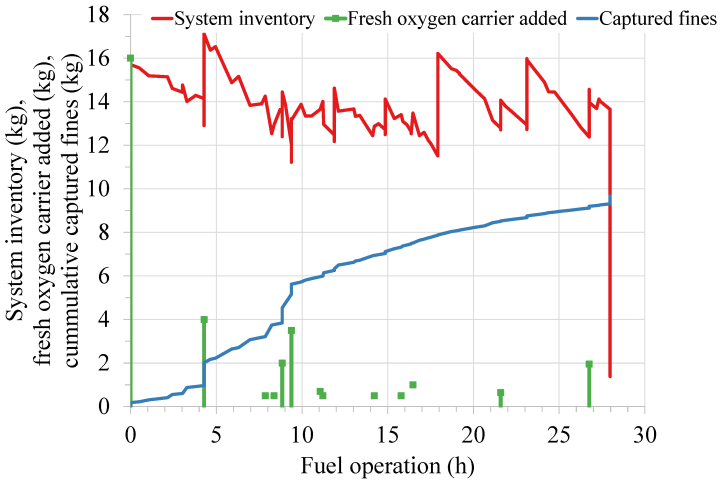

Figure 10: System inventory, fresh oxygen carrier added, cumulative captured fines as a function of fuel operation time in the 10 kW unit.

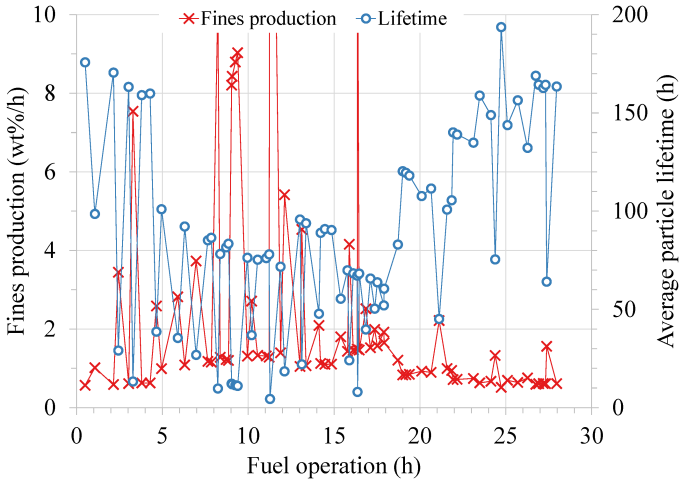

Figure 11: Fines production rate and estimated average particle lifetime as a function of fuel operation time in the 10 kW unit.

4 Summary and Conclusions

LD slag is an industrial by-product that is produced in very large amounts, while its use is limited. Thus, the cost of an oxygen carrier material for deployment in chemical looping applications, with respect to both raw material cost and cost of production, is potentially very low. LD slag was crushed, sieved and heat treated, before it was used for investigations in two small-scale chemical-looping reactor systems; 1) a unit with a nominal fuel input of 300 Wth, which was used with gaseous fuels syngas and methane for a total of 20 h with fuel operation, and 2) a unit with a nominal fuel input of 10 kWth, where investigations were conducted for a total of 28 h with three different biomass-based, solid fuels.

In the 300 W unit, the material was activated during the first couple of hours with addition of syngas. During activation, the material developed CLOU properties, i.e., the ability to release oxygen to the gas phase, and the CO_2 yield increased notably. Very high degrees of syngas conversion were achieved, i.e., CO_2 yields of up to 99.9 % at a specific fuel-reactor bed masses as low as 280 kg/MW_{th} and at a temperature of 900 °C. Methane conversion was far from complete, i.e., 60 % at most at 280 kg/MW_{th} and 950 °C, but still high compared to manganese ore-based oxygen carriers tested in this unit.

During chemical-looping combustion in the 10 kW unit, CO_2 yields of 75-82 % were achieved with all three fuels tested, while carbon leakage was very low in most cases, i.e., below 1 %. In one case

when wood char was used as fuel, a CO_2 yield of 92 % was reached, however, at a low fuel input, i.e., 1.8 kW_{th}. The carbon fraction of C_2-species in the fuel reactor was usually below 2.5 % and no C_3-species were detected. The oxygen carrier lifetime was estimated to be about 110-170 h, without taking into account effects of interaction with ash components.

During part of the investigation in the 10 kW unit the experimental parameters were adjusted to achieve chemical-looping gasification rather than chemical-looping combustion. For a gasification process, high fractions of H_2, CO and possibly CH_4 are desirable, while carbon leakage to the air reactor as well as the flue gas contents of char and tar should be as low as possible. Generally, the heating value of the cleaned product gas should be as high as possible. Not so surprisingly, black pellets and wood pellets, i.e., fuels with a high volatiles content, are more suitable for chemical-looping gasification than wood char. During chemical-looping gasification with black pellets as fuel, the dry flue gas consisted mostly of H_2, followed by CO_2, CO, CH_4 and C_2-species, not counting N_2. This raw gas is suitable for further processing towards a desired product.

The following conclusions can be drawn from the investigation conducted.

- LD slag is an industrial by-product, which is available in huge quantities and for which there is currently a very limited demand. To be used as oxygen carrier in a chemical-looping process, essentially, only crushing is required. Therefore, it should be much cheaper to produce than oxygen carrier materials based on minerals and ores.
- LD slag-based oxygen carrier develops CLOU properties during the initial hours of fuel operation, i.e., about 85 redox cycles. During that period its fuel conversion properties improve significantly.
- With LD slag-based oxygen carrier, 99.9 % conversion of CO to CO_2 is possible.
- With high-volatile fuels, i.e., black pellets and wood pellets, no C_3-hydrocarbons were detected in the fuel reactor fuel gas. With a low-volatile fuel, i.e., wood char, neither C_2- nor C_3-hydrocarbons were detected.
- Carbon leakage to the air reactor was low, in most cases below 1 % of the fuel carbon, so that high carbon capture efficiencies should be feasible.
- During chemical-looping gasification operation with high-volatile fuels, i.e., black pellets and wood pellets, a raw gas was produced that contained mostly hydrogen and that should be feasible for further processing towards a desired gas blend.
- Based on fines production, the particle lifetime was estimated to be 110-170 h. In a conventional CFB combustor this lifetime would correspond to a bed regeneration rate of about 5-8 kg/MWh, which is close to conventional regeneration rates and should therefore be feasible.

5 Acknowledgement

This work was carried out as part of the OxyCar-FBC project, which is conducted within the framework of ERA-NET Bioenergy and funded by the Swedish Energy Agency (P43936-1). This project has received additional support from a grant of the Swedish Energy Agency (P43220-1). The contribution of SSAB Merox AB in the preparation of LD slag is also acknowledged.

6 References

[1] Lyngfelt A., Leckner B. and Mattisson T. *A fluidized-bed combustion process with inherent CO_2 separation; application of chemical-looping combustion*. Chemical Engineering Science: 56, pp.3101-3113, 2001.

[2] Adánez J., Abad A., García-Labiano F., Gayán P. and de Diego L.F. *Progress in chemical-looping combustion and reforming technologies*. Progress in Energy and Combustion Science: 38, pp.215-282, 2012.

[3] Imtiaz Q., Hosseini D. and Müller C.R. *Review of Oxygen Carriers for Chemical Looping with Oxygen Uncoupling (CLOU): Thermodynamics, Material Development, and Synthesis*. Energy Technology: 1, pp.633-647, 2013.

[4] Lyngfelt A. and Linderholm C. *Chemical-Looping Combustion of Solid Fuels – Status and Recent Progress*. Energy Procedia: 114, pp.371-386, 2017.

[5] Linderholm C., Lyngfelt A., Cuadrat A. and Jerndal E. *Chemical-looping combustion of solid fuels - Operation in a 10 kW unit with two fuels, above-bed and in-bed fuel feed and two oxygen carriers, manganese ore and ilmenite*. Fuel: 102, pp.808-822, 2012.

[6] Moldenhauer P., Sundqvist S., Mattisson T. and Linderholm C. *Chemical-looping combustion of synthetic biomass-volatiles with manganese-ore oxygen carriers*. International Journal of Greenhouse Gas Control: 71, pp.239-252, 2018.

[7] Schmitz M., Linderholm C., Hallberg P., Sundqvist S. and Lyngfelt A. *Chemical-Looping Combustion of Solid Fuels Using Manganese Ores as Oxygen Carriers*. Energy and Fuels: 30, pp.1204-1216, 2016.

[8] Linderholm C., Schmitz M., Biermann M., Hanning M. and Lyngfelt A. *Chemical-looping combustion of solid fuel in a 100kW unit using sintered manganese ore as oxygen carrier*. International Journal of Greenhouse Gas Control: 65, pp.170-181, 2017.

[9] Rydén M., Leion H., Mattisson T. and Lyngfelt A. *Combined oxides as oxygen-carrier material for chemical-looping with oxygen uncoupling*. Applied Energy: 113, pp.1924-1932, 2014.

[10] Källén M., Rydén M., Lyngfelt A. and Mattisson T. *Chemical-looping combustion using combined iron/manganese/silicon oxygen carriers*. Applied Energy: 157, pp.330-337, 2015.

[11] Wang P., Leion H. and Yang H. *Oxygen-Carrier-Aided Combustion in a Bench-Scale Fluidized Bed*. Energy and Fuels: 31, pp.6463-6471, 2017.

[12] Keller M., Leion H., Mattisson T. and Thunman H. *Investigation of natural and synthetic bed materials for their utilization in chemical looping reforming for tar elimination in biomass-derived gasification gas*. Energy and Fuels: 28, pp.3833-3840, 2014.

[13] Johnsson F., Vrager A. and Leckner B. *Solids flow pattern in the exit region of a CFB-furnace - influence of exit geometry*. in *Fifteenth International Conference on Fluidized Bed Combustion*, Savannah, GA, USA, 1999.

[14] Kunii D. and Levenspiel O. *Fluidization engineering*. Butterworth-Heinemann, Boston, MA, USA, 1991.

[15] Moldenhauer P., Serrano A., García-Labiano F., De Diego L.F., Biermann M., Mattisson T. and Lyngfelt A. *Chemical Looping Combustion of Kerosene and Gaseous Fuels with a Natural and a Manufactured Mn-Fe-based Oxygen Carrier*. submitted for publication: 2018.

[16] Rydén M., Moldenhauer P., Lindqvist S., Mattisson T. and Lyngfelt A. *Measuring attrition resistance of oxygen carrier particles for chemical looping combustion with a customized jet cup*. Powder Technology: 256, pp.75-86, 2014.

[17] Lyngfelt A. and Leckner B. *A 1000 MW_{th} boiler for chemical-looping combustion of solid fuels – Discussion of design and costs*. Applied Energy: 157, pp.475-487, 2015.